

SIMULATIONS OF LONG-RANGE BEAM-BEAM COMPENSATION IN LHC

H.J. Kim, T. Sen, FNAL, Batavia, IL 60510, USA

Abstract

The compensation of long-range beam-beam interactions with current carrying wires in the Large Hadron Collider (LHC) is studied by multi-particle tracking. In the simulations, we include the effect of long-range collisions together with the nonlinearities of IR triplets, sextupoles, and head-on collisions. The model includes the wires placed at the locations reserved for them in the LHC rings. We estimate the optimal parameters of a wire for compensating the parasitic beam-beam force by long-term simulations of beam lifetime.

INTRODUCTION

Long-range beam-beam interactions are known to cause emittance growth or beam loss in the Tevatron and are expected to deteriorate beam quality in the LHC. Increasing the crossing angle to reduce their effects has several undesirable effects, the most important of which is a lower luminosity due to the smaller geometric overlap. For the LHC, a wire compensation scheme has been proposed to compensate the long-range interactions by applying external electromagnetic forces [1]. At large beam-beam separation, the electromagnetic force which a beam exerts on individual particles of the other beam is proportional to $\frac{1}{r}$, which can be generated and canceled out by the magnetic field of a current-carrying wire. However, several issues need to be resolved for efficient compensation. With the present bunch spacing, there are about 30 long-range interactions on both sides of an interaction point (IP). The beam-beam separation distance varies from 6.3σ to 12.6σ . The resulting beam-beam force is not identical to that generated by a single or multiple wire(s). The average phase advance between the location of the wire to the location of the long-range interaction points is about 3° , this may impact the compensation efficiency. In this paper, we have studied the dynamic aperture, the frequency diffusion map, and the particle loss for different wire currents and separation distances in order to investigate the effectiveness of the wire compensation.

MODEL

We apply a weak-strong model to study the long-range interactions and their compensation with current carrying wires. In the tracking code BBSIMC [2], the transverse and longitudinal motion of particles is calculated by linear transfer maps between nonlinear elements at which the nonlinear forces are exerted on the particles. We adopt the weak-strong model to treat the beam-beam interactions. The strong bunch is divided into slices in a longitudinal

Table 1: LHC parameters at proton-proton collision. The subscript $ip\{1,5\}\{left,right\}$ stands for the wire location.

quantity	unit	proton beam
energy, γ	TeV/n	7
bunch intensity	10^{11}	1.15
bunch spacing	ns	25
crossing angle	μrad	284
$\epsilon_{x,y}(95\%)$	mm mrad	22.5
(β_x^*, β_y^*)	m	(0.56, 0.59)
(ν_x, ν_y)		(64.31, 59.32)
(ξ_x, ξ_y)		(2, 2)
\mathcal{A}_B	eV·s	8.7
$\sigma_{\Delta p/p}$		1.13×10^{-4}
σ_z	m	7.55×10^{-2}
$I_w L_w$	Am	82.8
wire location from IP	m	104
$(\beta_x, \beta_y)_{ip1_left}$	m	(1783, 1792)
$(\beta_x, \beta_y)_{ip1_right}$	m	(1792, 1783)
$(\beta_x, \beta_y)_{ip5_left}$	m	(1783, 1792)
$(\beta_x, \beta_y)_{ip5_right}$	m	(1792, 1783)

direction to consider the finite bunch length effect of the beam-beam interaction. In the simulations, we applied 11 slices in the main IPs where the beta function is comparable with the bunch length. Each slice in a beam interacts with particles in the other beam in turn at the collision points. In case of the collision with crossing angle, the beam-beam force experienced by a test particle is not purely in the transverse direction, and depends on the longitudinal position as well. A Lorentz boost is applied for the crossing angle. It transforms a crossing angle collision in the laboratory frame to a head-on collision in the rotated and boosted frame which is called the head-on frame [3]. The transformation consists of a transformation from the accelerator coordinates to Cartesian coordinates, the Lorentz transformation, and again a backward transformation to the accelerator coordinates.

For a finite length of a wire embedded in the middle of a drift length L and tilted in pitch and yaw angles, the transfer map of a wire can be written as [4]

$$\mathcal{M}_w = S_{\Delta x, \Delta y} \odot T_{\theta_x, \theta_y}^{-1} \odot D_{L/2} \odot \mathcal{M}_k \odot D_{L/2} \odot T_{\theta_x, \theta_y},$$

where T_{θ_x, θ_y} represents the tilt of the coordinate system by horizontal and vertical angles θ_x, θ_y to orient the coordinate system parallel to the wire, $D_{L/2}$ is the drift map with a length $\frac{L}{2}$, \mathcal{M}_k is the wire kick integrated over a drift length, and $S_{\Delta x, \Delta y}$ represents a shift of the coordinate axes

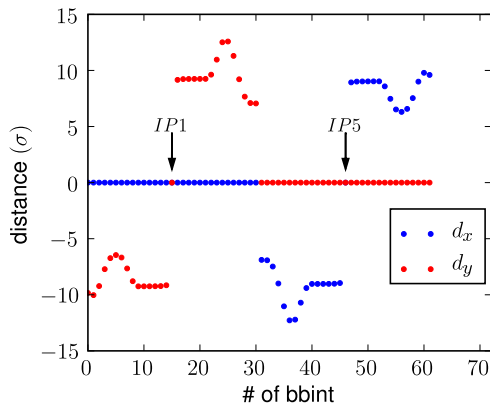


Figure 1: Beam-beam separation at IP 1 and 5.

Table 2: Wire Separation Distance Relative to the Center of a Proton Beam in Terms of rms Beam Size at Each Wire Location

wire	wire separation (σ)	
	horizontal	vertical
ip1_left	0	-8.56
ip1_right	0	+9.56
ip5_left	-9.33	0
ip5_right	+8.36	0

to make the coordinate systems after and before the wire agree. While particles at small r undergo a linear tune shift, the particles with $r \gg \sigma$ experience a $\frac{1}{r}$ force. The long-range effect is nonlinear and may vary from bunch to bunch if the the bunch pattern is asymmetric. A current carrying wire generates a magnetic force which is $\propto \frac{1}{r}$, the same as the long-range beam-beam force at large separations. The wire current required to compensate a long-range interaction is $(I_w L_w) = n_* q_* c$, where I_w is the wire current, and L_w its length. The integrated current for optimal tune compression is 82.8 Am. As shown in Fig. 1, the beam-beam separation distance normalized by the transverse rms bunch size varies from 6.3 σ to 12.6 σ and is asymmetric with respect to IPs. The beam-beam separations are averaged on both sides of IPs. The averaged separations are chosen as wire-beam separations which are summarized in Table 2. A wire is installed at 104 m away from the IP on each side of the IP. Hence, 4 wires are installed in the model.

SIMULATION RESULTS

The tune footprint provides useful information especially on the choice of working point and in finding the resonances spanned by the beam distribution. Figure 2 shows tune footprints from tracking single particles with initial amplitudes in the range 0-6 $\sigma_{x,y}$ for two cases: one without and one with the beam-beam compensation. At the nominal bunch intensity, the beam-beam parameter is $\xi \simeq 0.004$. The head-on collision introduces a large tune shift for the low amplitude particles. However, the long-

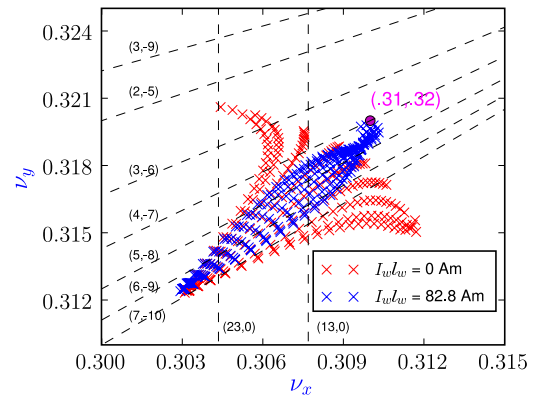


Figure 2: Plot of tune footprints for (red) without and (blue) with wire compensation. The no-wire case includes sextupoles, IR multipoles, head-on, and long-range interactions.

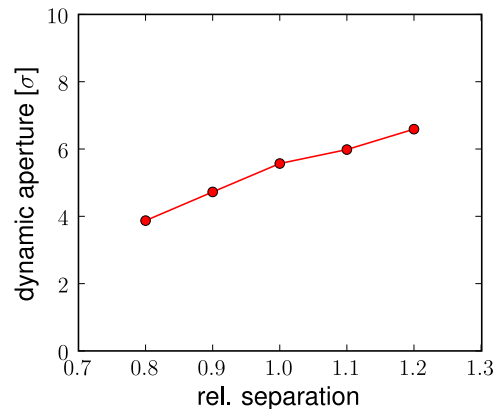


Figure 3: Plot of angle-averaged dynamic apertures according to wire separation distance with wire strength 82.8 Am. The separation is relative to values in Table 2.

range interactions affect higher amplitude particles, and increase the tune spread of the high amplitude particles. They can lead to emittance growth and beam loss. The footprint can be compressed to nearly the same spread as with the long-range interactions excluded, as shown in Fig. 2. This is achieved with a wire current 82.8 Am and the wire-beam separations shown in Table 2.

The wire-beam separation distance is one of major parameters which determine the performance of a wire compensator. Figure 3 shows the angle-averaged dynamic aperture for off-momentum particles with $3 \sigma_{\Delta p/p}$ for different wire-beam separations. The dynamic aperture calculated at different phase angles is the largest radial amplitude of particles that survive up to a certain time interval; in this simulation, 10^6 turns. In Fig. 3, the separation is represented by the one relative to values in Table 2. When the beam-beam compensation is not present, the dynamic aperture is around 8 σ . However, for a wide separation range, the dynamic aperture is smaller than 8 σ by about 2-4 σ . The dynamic aperture decrease linearly as the separation

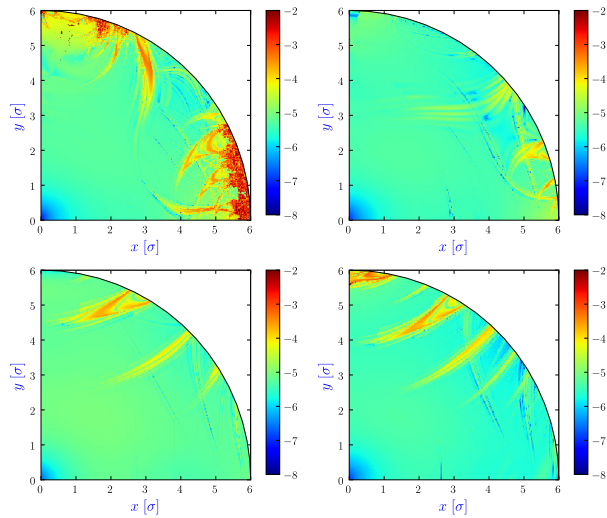


Figure 4: Plot of frequency diffusion map of betatron tunes for different wire separation distances: (top left) 0.8 times, (top right) 0.9 times, (bottom left) 1.0 times, and (bottom right) 1.1 times of values of Table 2. Wire strength is 82.8 Am. The tune change is logarithmically scaled by $\log\sqrt{\Delta\nu_x^2 + \Delta\nu_y^2}$.

decreases.

We have calculated frequency diffusion maps which represents the variation of the betatron tunes over two successive sets of the tunes. The variation can be quantified by $d = \log\sqrt{\Delta\nu_x^2 + \Delta\nu_y^2}$. A large tune variation is generally an indicator of reduced stability. Figure 4 shows the diffusion map of the betatron tune for particles with initial amplitudes in the range 0-6 $\sigma_{x,y}$ for different wire-beam separations. Contrary to the dynamic aperture in Fig. 3, the diffusion index is improved at a certain separation. For example, the 0.9 and 1.0 separations suppress the tune change especially at large amplitude beyond 4 σ , compared to the other separation. However, the small amplitude particles are unaffected by the beam-beam compensation.

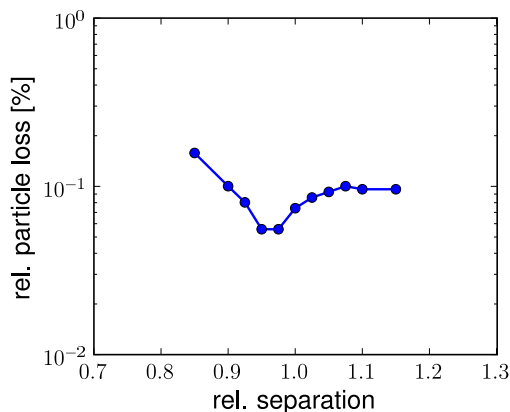


Figure 5: Plot of particle loss according to wire-beam separation distance with wire strength 82.8 Am. The separation is relative to values in Table 2.

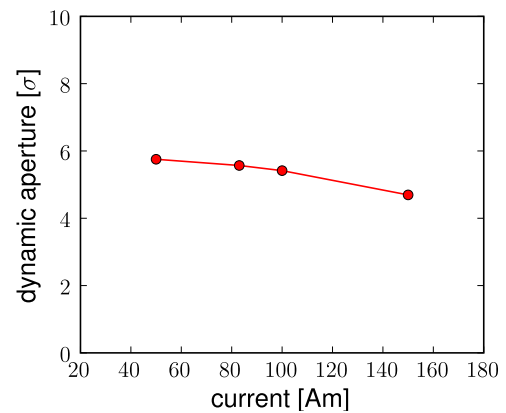


Figure 6: Plot of dynamic apertures according to wire current at fixed separation as shown in Table 2.

Figure 5 shows the results of particle loss in 1×10^6 turns for different wire-beam separations. We directly see the minimum particle loss between 0.9 and 1.0 separations. The particle loss saturates at large separation while there is a sharp increase of particle loss at small separation. The dependency of the beam loss on wire-beam separation is consistent with that of the frequency diffusion.

For different wire currents, we see the effects of wire compensation on the dynamic aperture as shown in Fig. 6. The current is varied from 40 Am to 150 Am which corresponds to 0.5 - 2 times 82.8 Am. The dynamic aperture stays roughly constant up to 100 Am, and falls down to 4.5 σ . The difference of the dynamic apertures between 40 Am and 150 Am is about 1 σ which is small compared to that with the separation change as shown in Fig. 3.

SUMMARY

In this paper, we investigated the effects of wire parameters, i.e, wire current and wire-beam separation, on the nominal LHC using weak-strong simulations. The results show that the particle loss is minimized at the wire separation between 0.9 and 1.0 of the reference separation. The separation corresponds to the one where the tune change of large amplitude particles is reduced. The dynamic aperture results show that the beam dynamics are more sensitive to the wire-beam separation than the wire current.

ACKNOWLEDGMENTS

This work was supported by the US-LARP collaboration which is funded by the US Department of Energy.

REFERENCES

- [1] J.P. Koutchouk, LHC Project Note 223, CERN (2000).
- [2] H.J. Kim et al., Phys. Rev. ST Accel. Beams 12, 031001 (2009).
- [3] K. Hirata et al., KEK Preprint 92-117 (1992).
- [4] B. Erdelyi and T. Sen, Fermilab-TM-2268-AD (2004).